

# Recurrence network approach to a phase space of a time-delay system

D. V. Senthilkumar<sup>†‡</sup>, N. Marwan<sup>‡</sup> and J. Kurths<sup>‡,\*</sup>

<sup>†</sup>Centre for Dynamics of Complex Systems, University of Potsdam, 14469 Potsdam, Germany

<sup>‡</sup>Potsdam Institute for Climate Impact Research, 14473 Potsdam, Germany

\* Institute for Physics, Humboldt University, 12489 Berlin, Germany

Email: senthil@pik-potsdam.de, marwan@pik-potsdam.de, kurths@pik-potsdam.de

**Abstract**—An interesting potential approach for nonlinear time series analysis by exploiting the analogy between the recurrence matrix, representing the recurrences in phase space, and the adjacency matrix of a complex network to characterize and analyze the dynamical transitions in the phase space of complex systems is being emerging. In this work, we present our preliminary results by applying this method to a high dimensional phase space of a time-delay system.

## 1. Introduction

Among modern data analysis techniques recurrence analysis has its unique advantages and is being used as a potential tool for time series analysis in almost all branches of science and technology [1]. The analogy between the recurrence matrix and the adjacency matrix has recently provoked a flurry of investigations in employing complex network measures to recurrences in phase space to analyse and characterize dynamical transitions in phase space in terms of network topology (cf.[2, 3, 4, 5, 6, 7]).

Recently, the network measures, namely link density ( $\rho$ ), average path length ( $L$ ) and clustering coefficient ( $C$ ), along with the recurrence quantification analysis (RQA), namely maximal diagonal line length ( $L_{max}$ ) and laminarity ( $LAM$ ) are estimated to capture the dynamical transitions in the well-known logistic map [2], as shown in Fig. 1, in terms of these measures. The dotted lines in these figures corresponds to the four different dynamical regimes (i) period-3 window at  $a = 3.830$ , (ii) band merging at  $a = 3.679$ , (iii) cross points of supertrack functions at  $a = 3.791$  and (iv) outer crisis at  $a = 4$ , which has been analysed in detail [2].

As a natural extension of these studies to high dimensional phase space, we have applied the above measures to a time-delay system, essentially an infinite-dimensional system, and discuss our preliminary results and the difficulties involved in it. In particular we consider a piecewise linear time-delay system and apply these measures to analyse the dynamical transitions in such a high-dimensional phase space.

The plan of the paper is as follows. In Sec. 2, we introduce the model system and discuss briefly about its dynamical properties. We will point out the measures that have employed in Sec. 3 We will present our preliminary results and discuss the practical difficulty involved in analyzing

such a high dimensional phase space in Sec. 4. Finally, in Sec. 5, we present our summary and conclusion.

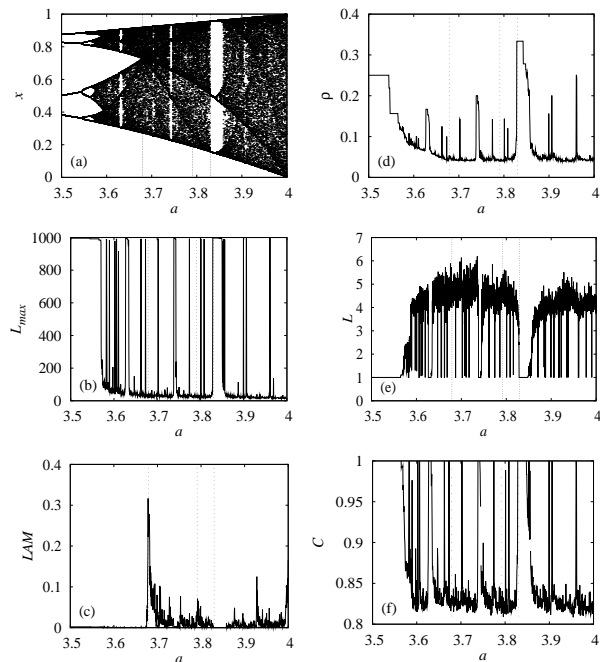


Figure 1: (a) Bifurcation diagram of the logistic map. Selected RQA measures: (b) maximal diagonal line length  $L_{max}$  and (c) laminarity  $LAM$ , as well as complex network measures: (d) link density  $\rho$ , (e) average path length ( $L$ ) and (f) clustering coefficient ( $C$ ).

## 2. Scalar piecewise linear time-delay system

We consider the following scalar first order delay differential equation represented as

$$\dot{x}(t) = -ax(t) + bf(x(t-\tau)) + c, \quad (1)$$

where  $a, b$  and  $c$  are parameters,  $\tau$  is the time-delay and  $f$  is an odd piecewise linear function defined as

$$f(x) = \begin{cases} 0, & x \leq -4/3 \\ -1.5x - 2, & -4/3 < x \leq -0.8 \\ x, & -0.8 < x \leq 0.8 \\ -1.5x + 2, & 0.8 < x \leq 4/3 \\ 0, & x > 4/3. \end{cases} \quad (2)$$

We have investigated the above system in detail including

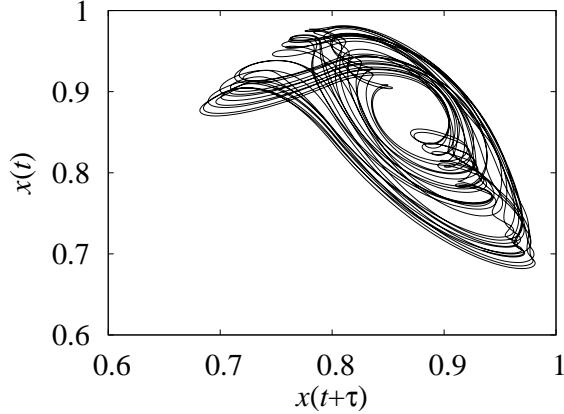


Figure 2: (a) The hyperchaotic attractor of the piecewise linear time-delay system, (1), for the choice of the parameters  $a = 1.0, b = 1.2, c = 0.001$  and  $\tau = 25.0$

linear stability analysis, bifurcation analysis and transient effects [8]. For the choice of the parameters  $a = 1.0, b = 1.2, c = 0.001$  and  $\tau = 25.0$  with the initial condition  $x(t) = 0.9, t \in (-\tau, 0)$ , the scalar piecewise linear time-delay system (1) exhibits hyperchaos (Fig. 2). The hyperchaotic nature of Eq. (1) is confirmed by the existence of multiple positive Lyapunov exponents. The first ten largest Lyapunov exponents for the above choice of the parameters as a function of delay time  $\tau \in (2, 29)$  are shown in Fig. 3, which are calculated using the procedure of Farmer [9]. In the following, we will briefly point out various RQA and complex network measures that we have estimated in this manuscript.

### 3. Measures of recurrence plots and complex networks

Recurrence plots (RPs) provide a visual impression of the trajectory of a dynamical system in phase space. Suppose that the time series  $\{X_i\}_{i=1}^N$  representing the trajectory

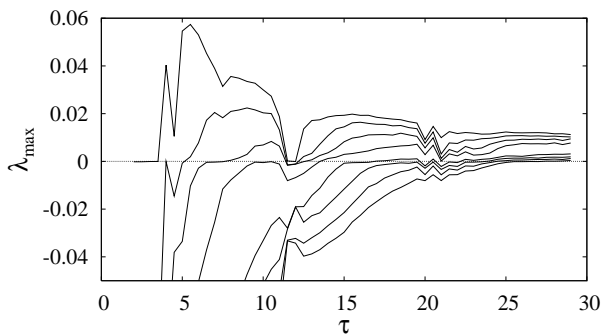


Figure 3: The first ten maximal Lyapunov exponents  $\lambda_{max}$  of the scalar time-delay system, (1), for the parameter values  $a = 1.0, b_1 = 1.2, c = 0.001, \tau \in (2, 29)$

of a system in phase space is given, with  $X_i \in \mathbb{R}^d$ . The RP efficiently visualises recurrences and can be formally expressed by the matrix

$$\mathbb{R}_{i,j} = \Theta(\epsilon - \|X_i - X_j\|), \quad i, j = 1, \dots, N, \quad (3)$$

where  $N$  is the number of measured points  $X_i$ ,  $\epsilon$  is a predefined threshold,  $\Theta$  is the Heaviside function and  $\|\cdot\|$  is the Euclidean norm. For  $\epsilon$ -recurrent states, that is for states which are in an  $\epsilon$ -neighbourhood, we have the following notion:

$$X_i \approx X_j \iff \mathbb{R}_{i,j} \equiv 1. \quad (4)$$

The graphical representation of the matrix  $\mathbb{R}_{i,j}$  is called recurrence plot (RP). The RP is obtained by plotting the recurrence matrix, Eq. (3), using different colors for its binary entries, for example by marking a black dot at the coordinates  $(i, j)$ , if  $\mathbb{R}_{i,j} \equiv 1$ , and a white dot, if  $\mathbb{R}_{i,j} \equiv 0$ . More details about the RPs and RQAs along with their applications can be found in [1]. Now, we will directly introduce the measures which we have used for our analysis:

1. Maximal diagonal length ( $L_{max}$ ) defined as

$$L_{max} = \max(\{l_i\}_{i=1}^{N_l}), \quad (5)$$

where,  $l$  is length of diagonal lines and  $N_l$  is their total number.

2. Laminarity defined as

$$LAM = \frac{\sum_{v=v_{min}}^N v p(v)}{\sum_{v=1}^N v p(v)}, \quad (6)$$

where  $p(v)$  is the distribution of the vertical lines of at least length  $v$ .

3. Link density given as

$$\rho = \frac{1}{N(N-1)} \sum_{i,j=1}^N A_{i,j}, \quad (7)$$

corresponding to the global recurrence rate and  $A_{i,j} = \mathbb{R}_{i,j} - \delta_{i,j}$ , where  $\delta_{i,j}$  is the Kronecker delta.

4. Clustering coefficient,  $C = \sum_v C_v / N$ , where the local clustering coefficient  $C_v$  is defined as

$$C_v = \frac{\sum_{i,j=1}^N A_{v,i} A_{i,j} A_{j,v}}{k_v(k_v - 1)}, \quad (8)$$

where  $k_v = \sum_{i=1}^N A_{v,i}$  is the degree centrality giving the number of neighbours of node  $v$ .

5. The average length of shortest path between all pairs of nodes is given by the average path length

$$L = \frac{1}{N(N-1)} \sum_{i,j=1}^N d_{i,j}, \quad (9)$$

where  $d_{i,j}$  is the shortest path connecting the nodes  $i$  and  $j$ .

More details and discussions on these measures and their application to understand the dynamical transitions in the phase space of complex systems can be found in Refs. [2, 3, 4].

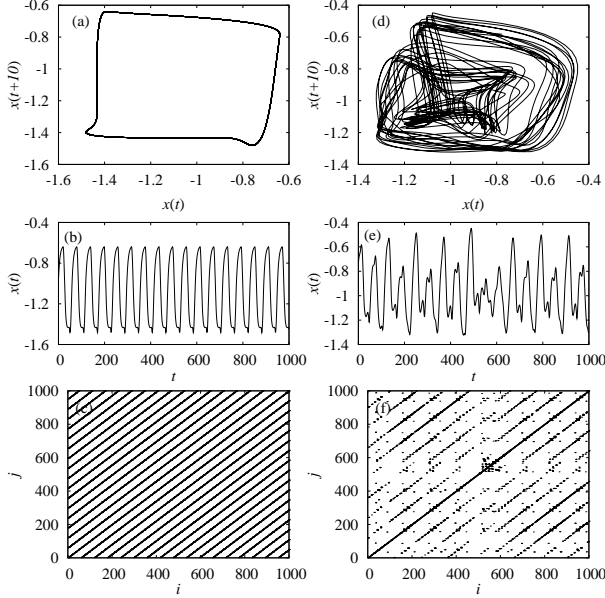


Figure 4: (a-c) Periodic attractor, its time series and its corresponding RP, respectively, for the value of  $c = -0.1$  and (d-f) hyperchaotic attractor, its time series and its corresponding RP, respectively, for the value of  $c = -0.06$ .

#### 4. Application to the time-delay system

To investigate the structural changes in the above mentioned measures corresponding to the dynamical transitions in the phase space of the piecewise linear time-delay system, we consider the same parameter values ( $a = 0.16$ ,  $b = 0.2$  and  $\tau = 25.0$ ) and the bifurcation diagram as in Fig. 4 of Ref. [8]. In our simulations, we have left sufficiently large transients and analysed time series of length  $N = 100,000$ . We have fixed the integration time step as  $\Delta t = 0.01$ , sampling interval as  $\Delta t_s = 100$  and the threshold value for  $\epsilon = 0.13\sigma$ , where  $\sigma$  is the standard deviation. The periodic attractor projected in the phase space ( $x(t)$ ,  $x(t + \hat{\tau})$ ) with  $\hat{\tau} = 10$  and its corresponding time series for the value of  $c = -0.1$  are shown in Figs. 4a and 4b, respectively. Similarly, the chaotic attractor and its corresponding time series for  $c = -0.06$  are shown in Figs. 4d and 4e, respectively. The RPs of the periodic (Fig. 4a) and the chaotic (Fig. 4d) attractors are shown in Figs. 4c and 4f, respectively.

The bifurcation diagram in the range of the control parameter  $c \in (-0.1, -0.05)$  is shown in Fig. 5a. We have calculated the values of the measures, mentioned in Sec. 3, corresponding to the attractors in the phase space ( $x(t)$ ,  $x(t + \hat{\tau})$ ) with  $\hat{\tau} = 10$ . Equivalently one may also consider other phase variables  $x(t + M\Delta t)$ , where  $M = \frac{\tau}{\Delta t} = \frac{25}{0.01} = 2500$

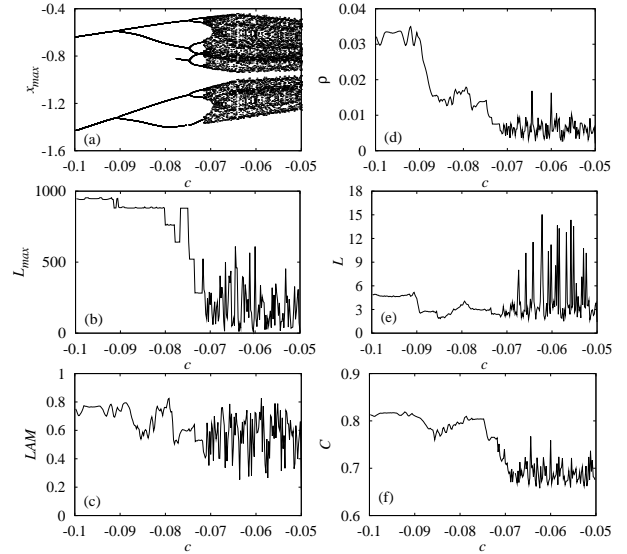


Figure 5: (a) Bifurcation diagram of the scalar piecewise linear time-delay system for the parameter values  $a = 0.16$ ,  $b_1 = 0.2$ ,  $\tau = 25$  and  $c \in (-0.1, -0.05)$ . Selected RQA measures: (b) maximal diagonal line length  $L_{max}$  and (c) laminarity  $LAM$ , as well as complex network measures: (d) link density  $\rho$ , (e) average path length ( $L$ ) and (f) clustering coefficient ( $C$ ).

for the chosen values of the delay time  $\tau$  and the integration time step  $\Delta t$ . However, more attention have to be paid for choosing the threshold value of  $\epsilon$  to avoid other recurrences within the  $\epsilon$  neighbourhood due to the tangential motion, namely, the sojourn points. This plays a vital role in determining the resulting structures in the above measures.

The maximal diagonal line length ( $L_{max}$ ) is depicted in Fig. 5b as a function of  $c$  corresponding to the bifurcation diagram (Fig. 5a). As expected  $L_{max}$  is very large (nearly equal to the length of the considered time series after the sampling) in the periodic regimes. However,  $L_{max}$  does not acquire low values in the chaotic regime, when compared to the logistic map (Fig. 1b) as expected due to the highly disconnected diagonal lines in the RP for a chaotic attractor in general. Nevertheless, the scenario is different in the case of chaotic/hyperchaotic attractors of time-delay systems as such systems will have trajectories with large periods as confirmed by the long diagonal lines in the RP of the chaotic attractor (Fig. 4f). It is also to be accounted that small amplitude to the large value of  $L_{max}$  is also contributed by the sojourn points.

The laminarity ( $LAM$ ), illustrated in Fig. 5c, in the periodic regime should be almost around zero (as in Fig. 1c of Logistic map) as there should not be any clusters of recurrence points in the periodic regime. However the large values of  $LAM$ , throughout the range of  $c$  and in the periodic regime in particular, is due to the recurrence of a large number of tangential motions within the  $\epsilon$  neighbourhood. Due

to high dimensional phase space of the time-delay systems, the projection of the trajectory in certain phase space may remain static for long time, while it is evolving in some other phase space. This may be avoided by considering more number of phase space/variables in embedding, while constructing the recurrence matrix and choosing appropriate phase space.

The link density ( $\rho$ ), shown in Fig. 5d, quantifies the average phase space density. It acquired large values in the periodic regime and low values in the chaotic regime as expected corresponding to large recurrences in the periodic regime (Fig. 4a) and comparatively low recurrences in the chaotic regime (Fig. 4d). However, as mentioned earlier the sojourn points will have small contribution to the amplitude of  $\rho$ . The average shortest path length ( $L$ ) and the clustering coefficient ( $C$ ) are plotted in Figs. 5e and 5f, respectively. In the periodic regimes, the different periods correspond to different disconnected components, as they never occur at the same point in phase space, with each component being a fully connected network as each periodic trajectory/behavior represents the same state in the phase space. Hence  $L$  should acquire the value unity and  $C$  should take the largest possible value ( $C = 1$ ) in the periodic regime as in Figs. 1e and 1f, respectively, for the case of the Logistic map. The average shortest path length takes the small value and the clustering coefficient takes largest value in the periodic regime as can be seen in Figs. 5e and 5f, respectively. However,  $L$  is slightly above and  $C$  is less than unity in the periodic regime because of the presence of sojourn points. In chaotic regime,  $L$  acquires larger values and  $C$  takes lower values than in the periodic regime as expected.

## 5. Summary and Conclusion

We have presented our preliminary results by extending the concept of recurrence network to a high dimensional system, namely a scalar piecewise linear time-delay system. In particular, we have estimated some of the recurrence quantification and network measures based on the recurrences in the phase space of the time-delay system. We have found that these measures characterize and quantify dynamical transitions in high-dimensional state space similar to that observed in the well-known logistic map. However, applying the recurrence network concept to retrieve exactly the dynamical and the statistical properties involved in the high-dimensional state space is a difficult task. One has to carefully analyse the phase spaces of infinite-dimensional systems such as time-delay systems to choose more appropriate phase spaces, in which most of the dynamical transitions occur, to be considered in the embeddings to construct the recurrence matrix to avoid any artifact.

## Acknowledgments

DVS has been supported by Alexander von Humboldt Foundation. JK has been supported by his Humboldt-CSIR research award and EU project No. 240763 PHOCUS(FP7-ICT-2009-C).

## References

- [1] N. Marwan, M. C. Romano, M. Thiel and J. Kurths, "Recurrence plots for the analysis of complex systems," *Phys. Rep.*, vol.438, pp.237–329, 2007.
- [2] N. Marwan, J. F. Donges, Y. Zou, R. V. Donner and J. Kurths, "Complex network approach for recurrence analysis of time series," *Phys. Lett. A*, vol.373, pp.4246–4254, 2009.
- [3] R. V. Donner, Y. Zou, J. F. Donges, N. Marwan and J. Kurths, "Ambiguities in recurrence-based complex network representations of time series," *Phys. Rev. E*, vol.81, pp.015101(R)(1-4), 2010.
- [4] R. V. Donner, Y. Zou, J. F. Donges, N. Marwan and J. Kurths, "Recurrence networks—a novel paradigm for nonlinear time series analysis," *New J. Phys.*, vol.12, pp.033025(1-40), 2010.
- [5] X. Xu, J. Zhang and M. Small, "Superfamily phenomena and motifs of networks induced from time series," *Proc. Natl Acad. Sci. USA*, vol.105, pp.19601–19605, 2008.
- [6] Z. Gao and N. Jin, "Flow-pattern identification and nonlinear dynamics of gas-liquid two-phase flow in complex networks," *Phys. Rev. E*, vol.79, pp.066303(1-14), 2009.
- [7] Z. Gao and N. Jin, "Complex network from time series based on phase space reconstruction," *Chaos*, vol.19, pp.033137(1-12), 2009.
- [8] D. V. Senthilkumar and M. Lakshmanan, "Bifurcations and chaos in time delayed piecewise linear dynamical systems," *Int. J. Bifurcation and Chaos*, vol.15, pp.2895–2912, 2005.
- [9] J. D. Farmer, "Chaotic attractors of an infinite-dimensional dynamical system," *Physica D*, vol.4, pp.366–393, 1982.